6th International Conference on Computational and Mathematical Biomedical Engineering - CMBE2019
10–12 June 2019, Japan
P. Nithiarasu, M. Ohta, M. Oshima (Eds.)

ESTIMATION OF A COMPATIBLE CARDIAC CONDUCTION SYSTEM FROM DISCRETE ENDOCARDIAL TIME SAMPLES

Fernando Barber[1], Pau Romero[1], Peter Langfield[2,4], Miguel Lozano[1], Ignacio García-Fernández[1], Josselin Duchateau[2,3], Mélèze Hocini[2,3], Michel Haïssaguerre[2,3], Edward Vigmond[2,4], and Rafael Sebastian[1]

[1]CoMMLab, Universitat de Valencia, Burjassot, Valencia, Spain,
{fernando.barber,pau.romero,miguel.lozano, ignacio.garcia,
rafael.sebastian}@uv.es
[2]IHU Liryc, Electrophysiology and Heart Modeling Institute, Fondation Bordeaux Université,
Pessac-Bordeaux, France {peter.langfield,edward.vigmond}@u-bordeaux.fr
[3]Bordeaux University Hospital (CHU), Cardiac Electrophysiology and Cardiac Stimulation Team, Pessac,
France, {Josselin.Duchateau,meleze.hocini,michel.haissaguerre
}@chu-bordeaux.fr
[4]Univ. Bordeaux, IMB UMR 5251, F-33400 Talence, France,

SUMMARY

Reconstructing a patient-compatible Purkinje Network from electroanatomical maps is a challenging task, that could help improve models for electrophysiology simulation. In this study, we present a method to build a Purkinje network from estimated Purkinje-myocardial junctions, that is compatible with patient's electroanatomical map with an average error below 1ms. We carry out a simulation study to show the effect of PMJ density on the estimated times and Purkinje network morphology.

Key words: *cardiac conduction system, inverse estimation, electrophysiology personalization*

1 INTRODUCTION

The reconstruction of the ventricular cardiac conduction system (CCS) from patient-specific data is a challenging problem [1, 2]. High-resolution imaging techniques have allowed only the segmentation of proximal sections of the CCS from images acquired ex-vivo [6]. Some methods have already been presented to estimate the Purkinje Network (PKN) from electro-anatomical maps (EAMs) [4, 3]. In this paper, we present an algorithm that estimates a set of Purkinje-myocardial junctions (PMJs) from EAMs, and builds a PKN compatible with the the location and activation time of PMJs. The algorithm is tested on several PKN configurations, with simulated and clinical data. The results show that the set of PMJs built explains the observed activation map for different synthetic CCS configurations. The average error in the predicted activation time is below the amplitude of the error in the data.

2 MATERIAL AND METHODS

An EAM was acquired at Bordeaux University Hospital using the CARTO system (Webster Biosense) from a patient showing idiopatic ventricular fibrilation. Each sample acquired was postprocesed to obtain the local activation time (LAT) as the maximum negative deflection in monopolar and biopolar signals, and subsequently performing a manual validation, and filtering of samples that do not show spatio-temporal correspondence.

2.1 Algorithm

The goal of the algorithm is to find the PKN branching configuration that is able to reach all the estimated PMJs minimizing both the estimated LAT at the PMJ and the length of the whole PKN

Name	PMJs	PMJs<4.0	PMJs<1.0	Error at PMJs	Distance error	Error at mesh
PK6	1224	96.32%	84.23%	0.69 ± 0.6 ms	0.87 ± 1.32 mm	0.52 ± 0.3 ms
PK3	831	94.83%	79.42%	0.72 ± 0.6 ms	1.76 ± 2.61 mm	0.63 ± 0.5 ms
PK11	442	96.83%	88.20%	0.65 ± 0.6 ms	1.19 ± 1.39 mm	0.63 ± 0.5 ms
PK4	362	95.86%	78.45%	0.70 ± 0.6 ms	1.53 ± 1.58 mm	0.65 ± 0.5 ms
PK15	206	95.63%	80.58%	0.81 ± 0.7 ms	1.89 ± 2.06 mm	0.72 ± 0.8 ms

Table 1: Estimation of the PKN directly from the real PMJs.

structure. The endocardium is represented as a triangle mesh in a three-dimensional space, $\Omega \subset \mathcal{R}^3$. We have a set of estimated PMJs $\Theta = \{\theta_1, ..., \theta_n\} \subset \mathcal{V} \times \mathcal{R}^+$, where $\mathcal{V}$ is the set of vertices of Ω. For each PMJ $t_i \in \mathcal{R}^+$ is the estimated Local Activation Time (LAT) at the PMJ. A connected, acyclic graph Ξ represents the PKN. Every vertex in Ξ has an activation time according to the PKN and the propagation velocity. The terminal vertices of Ξ have to be locations of the estimated PMJs.

We build the estimated PKN iteratively. An initial branch Ξ_0, corresponding to the His bundle and Left Bundle Branch (LBB), is built before the algorithm generates any further branch. The initial branch starts always from a location determined by the user and expands to the apex through the septal wall following the shortest path [3]. Then, we process the PMJs ordered by LAT, starting by the earliest one. Therefore, we start building the PKN from the region closer to the LBB, which is expected to show smaller LAT errors due to the shorter path from the Atrioventricular Node (AVN). After step i, we have processed $i-1$ PMJs in Θ and have built an estimated tree Ξ^{i-1} that connects them. We pick θ_i and solve the Eikonal problem on Ω starting from θ_i to obtain the distance from the estimated PMJ to all the vertices on Ξ^{i-1}. Then, we try to connect the PMJ θ_i with Ξ using a geodesic that ends at a point $\xi_i \in \Xi^{i-1}$. The connection point is chosen so that it minimizes the difference between the activation time of θ_i through Ξ_i and the value of t_i. We use the constraint that the path cannot intersect the PKN created so far. We only connect θ_i with a new branch if the error is below a threshold. Once the iteration ends with the last θ_i, the process is restarted trying to connect the disregarded PMJs to the estimated PKN, using a larger threshold. The algorithm stops when all the PMJs have been connected to Ξ or when the error threshold reaches a predefined bound.

2.2 Experimental setup

We have built a series of synthetic PKNs on the geometry of a left ventricular endocardium reconstructed from MRI, using the stochastic method described in [5], and have generated the corresponding tissue activations. More information about the different PKN generated and some images can be found in [1]. For the evaluation of the algorithm, we have performed two sets of experiments. First, we have used the actual PMJs of each PKN to build an estimated PKN and compare it with the original. Second, we have simulated an EAM acquisition registering the activation time, according to the different PKNs, at a number of measurement points uniformly distributed. A Gaussian error is added to the actual LAT on the measurement points. We estimate the PMJs from this information using [1], which are used as the input data for our algorithm. In order to have a quantitative assessment of the algorithm we consider several measures of quality, summarized in Tables 1 and 2. We have considered: the number of nodes in Θ that have been successfully connected to Ξ (error $<$ 4.0ms); the mean absolute error of the activation time at PMJs θ_i according to the activation resulted from the propagation through the estimated PKN and a given conduction velocity, in ms; the average distance from the estimated branches and the real branches per branch subsegment.

3 RESULTS AND CONCLUSIONS

For the estimation of PKNs, we compared the results using real (Table 1) and estimated PMJs (Table 2) as input to the algorithm. As expected, the real PMJs yield smaller errors, and the PKN structure is better reproduced (see Fig. 1). The difference in LAT at PMJs when using the real PMJs is below $1ms$ for all scenarios, as it is the average errors after propagating the signal to all mesh nodes. The average distances between tree segments is less than $1mm$, due to the close match of real and estimated PKNs in most tree sections. In addition, around 95% of the PMJs can be connected to the three with an error

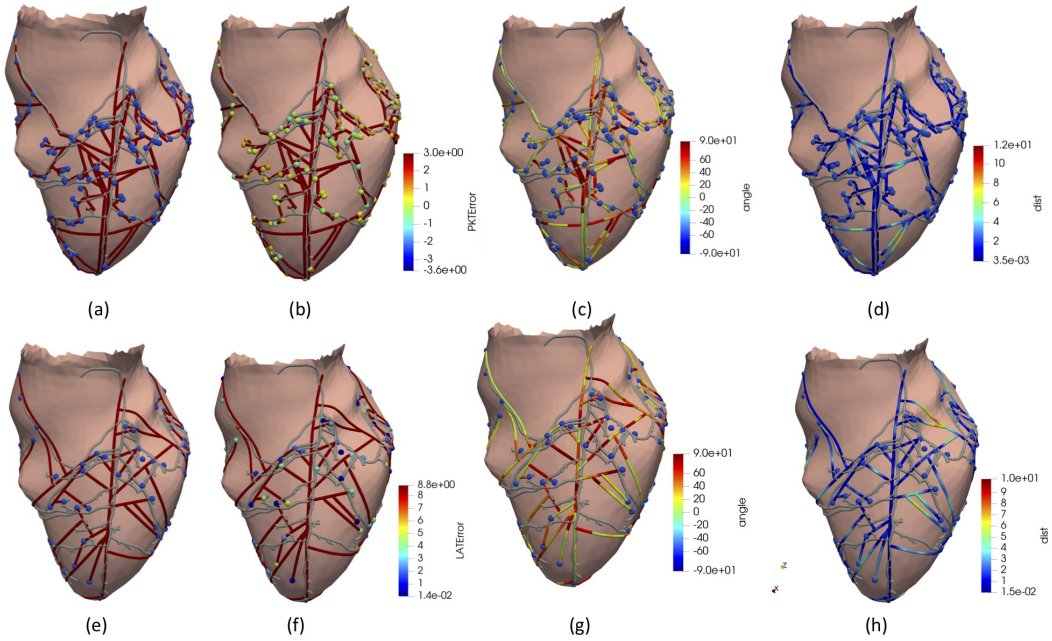

Figure 1: Graphical results for PK11 and $\sigma = 0.5$. The original PKN is depicted as a tubular structure in grey color, while PMJ are represented with spheres. First row correspond to estimated PKNs using the real PMJs, while second row are the PKN estimated from estimated PMJs (also included). PMJs in (b) and (f) are color coded to show the error (ms) when the estimated PKN is used. PKN in (c) and (d) show the differences in angle (degrees) between the real and the estimated PKN branches, while (d) and (h) show the distance (mm) between the elements of the real and the estimated PKN.

Name	PMJs	CV	PMJs<4.0	PMJs<1.0	Error at PMJs	Distance error	Error at mesh
PK6	114	1.1	76.32%	62.28%	0.79 ± 0.9ms	2.20 ± 2.7mm	1.67 ± 1.8ms
PK3	95	1.2	77.89%	60.00%	0.66 ± 0.7ms	2.11 ± 2.4mm	1.20 ± 1.4ms
PK11	111	1.0	81.98%	63.96%	0.76 ± 0.8ms	1.92 ± 1.8mm	1.40 ± 1.4ms
PK4	99	1.0	85.86%	69.70%	0.72 ± 0.6ms	2.17 ± 2.1mm	1.18 ± 1.2ms
PK15	83	1.1	79.52%	57.83%	0.72 ± 0.5ms	3.09 ± 3.6mm	1.38 ± 1.6ms

Table 2: Estimation of PKN from estimated PMJs and error $\sigma = 0.5ms$. Conduction velocities (CV) in m/s.

below $4.0ms$. When estimated PMJs are used to build the PKN, the conduction velocity in the PKN has to be estimated. Since we only have a subset of the PMJs, the algorithm tends to overestimate the conduction velocity (see Table 2 (CV)), where most cases have values above the real value of $1.0m/s$. The percentage of estimated PMJs successfully connected to the PKN decreases, due to errors in their location and activation time (note that error was inserted in the samples as described in [1]), but it is always above 75%. Although errors at PMJs are still below $1ms$ in all scenarios, the average error across the mesh increases to around $1.3ms$ due to the underestimation in the overall number of PMJs. The same explanation applies to the increase in distance error, since the low number of PMJs and associated branches in the estimated PKN leads to larger distances to the real PKN.

The estimation of PKN was carried out in an exemplary patient, based on the EAM data collected from the LV endocardium. The electrical signals were filtered and processed to detect LATs. A total of 210 samples manually validated, and projected to a reference endocardial surface mesh, were used as an input for the algorithm. The conduction velocities (CV) that produced a meaningful PKNs were in the range between 2.5 and 4.0 m/s, which are within a physiological range, although overestimation was expected since only a total of 22 PMJs was estimated. This low number was obtained because estimated PMJs were discarded if they did not meet criteria related to correlation with sample points. Best case was obtained using a CV of 3m/s (see Table 3), with a full connection of PMJs and an average error of $0.27ms$ at PMJs. Since we do not have ground truth data for LAT at all the mesh point (CARTO data is interpolated), we could not obtain the associated error. The structure of the estimated PKN changed depending on the CV used, as can be observed in Fig. 2, since the path

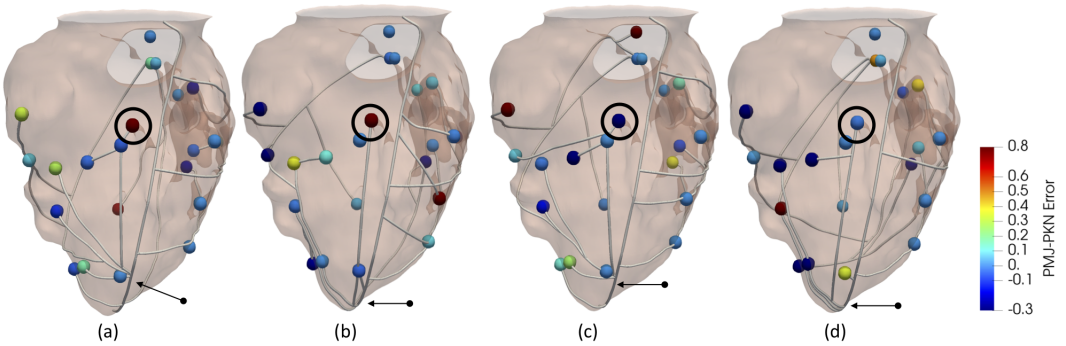

Figure 2: PKN Estimated from patient's EAM using different conduction velocities (CVs). CVs were (a) 2.5m/s, (b) 3.0m/s, (c) 3.2m/s, and (d) 4.0m/s. As can be observed, the structure of the PKN and the errors at the PMJs change depending on the conduction velocity chosen.

CV (m/s)	2.5	3.0	3.2	3.5	4.0
PMJs<4.0	100.0%	100.0%	95.5%	94.4%	100.0%
PMJs<1.0	72.2%	83.3%	50.0%	38.9%	54.6%
Error at PMJs	0.33 ± 0.5ms	0.27 ± 0.3ms	0.99 ± 1.5ms	0.69 ± 1.19ms	0.64 ± 1.0ms

Table 3: Estimation of the PKN from EAM data.

length from the atrio-ventricular node to a given PMJ is affected by this parameter. Overall, the errors obtained at PMJs are small enough to apply this method to estimate the PKN for patient-specific cardiac modeling. Due to the under estimation of PMJs, the CV in PKN is expected to be overestimated, as well as the overall activation of the endocardium. One of the most important drawbacks of the method is the dependence on the estimation of LATs at PMJs, which have to be carefully reviewed to avoid spatio-temporal inconsistent maps.

REFERENCES

[1] Fernando Barber, Ignacio García-Fernández, Miguel Lozano, and Rafael Sebastian. Automatic estimation of purkinje-myocardial junction hot-spots from noisy endocardial samples: A simulation study. *International Journal for Numerical Methods in Biomedical Engineering*, 34(7):e2988, 2018.

[2] Fernando Barber, Miguel Lozano, Ignacio García-Fernández, and Rafael Sebastian. Inverse estimation of terminal connections in the cardiac conduction system. *Mathematical Methods in Applied Sciences*, 41(6):2340–2349, 2018.

[3] Rubén Cárdenes, Rafael Sebastian, David Soto-Iglesias, Antonio Berruezo, and Oscar Camara. Estimation of purkinje trees from electro-anatomical mapping of the left ventricle using minimal cost geodesics. *Med Image Anal*, 24(1):52–62, Aug 2015.

[4] Simone Palamara, Christian Vergara, Elena Faggiano, and Fabio Nobile. An effective algorithm for the generation of patient-specific purkinje networks in computational electrocardiology. *Journal of Computational Physics*, 283(Supplement C):495 – 517, 2015.

[5] Rafael Sebastian, Viviana Zimmerman, Daniel Romero, Damian Sanchez-Quintana, and Alejandro F Frangi. Characterization and modeling of the peripheral cardiac conduction system. *IEEE Trans Med Imaging*, 32(1):45–55, Jan 2013.

[6] Robert S Stephenson, Andrew Atkinson, Petros Kottas, Filip Perde, Fatemeh Jafarzadeh, Mike Bateman, Paul A Iaizzo, Jichao Zhao, Henggui Zhang, Robert H Anderson, Jonathan C Jarvis, and Halina Dobrzynski. High resolution 3-dimensional imaging of the human cardiac conduction system from microanatomy to mathematical modeling. *Sci Rep*, 7(1):7188, Aug 2017.